Hindawi
International Journal of Antennas and Propagation
Volume 2017, Article ID 6790504, 12 pages
https://doi.org/10.1155/2017/6790504

Research Article

Path-Loss Channel Models for Receiver Spatial Diversity Systems at 2.4 GHz

Abdulmalik Alwarafy,[1] Ahmed Iyanda Sulyman,[1] Abdulhameed Alsanie,[1] Saleh A. Alshebeili,[1,2] and Hatim M. Behairy[3]

[1]*Department of Electrical Engineering, King Saud University, Riyadh, Saudi Arabia*
[2]*KACST-TIC in RF and Photonics for the e-Society (RFTONICS), Department of Electrical Engineering, King Saud University, Riyadh, Saudi Arabia*
[3]*National Center for Electronics and Photonics Technology, King Abdulaziz City for Science and Technology, Riyadh, Saudi Arabia*

Correspondence should be addressed to Abdulmalik Alwarafy; 437106913@student.ksu.edu.sa

Received 27 January 2017; Revised 21 March 2017; Accepted 23 March 2017; Published 13 April 2017

Academic Editor: Ikmo Park

This article proposes receiver spatial diversity propagation path-loss channel models based on real-field measurement campaigns that were conducted in a line-of-site (LOS) and non-LOS (NLOS) indoor laboratory environment at 2.4 GHz. We apply equal gain power combining (EGC), coherent and noncoherent techniques, on the received signal powers. Our empirical data is used to propose spatial diversity propagation path-loss channel models using the log-distance and the floating intercept path-loss models. The proposed models indicate logarithmic-like reduction in the path-loss values as the number of diversity antennas increases. In the proposed spatial diversity empirical path-loss models, the number of diversity antenna elements is directly accounted for, and it is shown that they can accurately estimate the path-loss for any generalized number of receiving antenna elements for a given measurement setup. In particular, the floating intercept-based diversity path-loss model is vital to the 3GPP and WINNER II standards since they are widely utilized in multi-antenna-based communication systems.

1. Introduction

Diversity is a robust communication technique utilized in modern wireless systems to improve the quality of the received signals and to ensure a better link performance. It is basically used to mitigate the effects of fading experienced by a receiver in flat fading channels. The general concept of diversity is implemented through using diverse communication channels each with different operating characteristics. This will guarantee better signal quality and thus better bit error rate (BER) performance, better signal-to-noise-ratio (SNR), and better signal coverage. The most commonly used implementation approaches for diversity systems in wireless transmissions are frequency diversity, spatial diversity, time diversity, coding diversity, and polarization diversity. Each of these approaches achieves a significant improvement in the wireless link performance [1]. The most efficient and widely used implementation in modern wireless communication systems however is the spatial diversity [1]. For example, the multiple-input multiple-output (MIMO) communication systems employed multiple spatial antenna elements at both the transmitter (TX) and the receiver (RX) sides to boost signal level and hence to increase the SNR. These MIMO-based systems are now implemented in a wide variety of wireless systems such as the wireless local area networks WLANs (i.e., IEEE 802.11n/ac), the WiMAX, and the Fourth-Generation Long Term Evolution (4G-LTE) for cellular systems. The most commonly utilized combining techniques in spatial diversity are selection combining (SC), equal gain combining (EGC), and maximal ratio combining (MRC) schemes [1–4]. The SC only requires an individual receiver and a basic phasing circuitry for each diversity branch. In the EGC, the weights of each branch are set to unity and the signals of each branch are combined either without cophasing (noncoherently) or with cophasing (coherently). In MRC, however the signals from all the diversity branches are

weighted according to their individual SNRs, cophased, and then summed. The SNR enhancements over a flat Rayleigh fading channel as a function of the number of diversity antennas combined for these three techniques reveal that EGC has slightly less SNR gain enhancement compared to MRC [1]. However, our measurement work here uses the EGC scheme since it is moderate in complexity, as it only needs information about the phases of the signals. The MRC, on the other hand, is more complex to implement since an estimation of both phases and amplitudes of the signals must be realized [2, 5], which is difficult to be achieved with our equipment.

There are many works that have introduced path-loss models for single-input single-output (SISO) schemes, such as the works in [6, 7]. However, despite the implementation of spatial diversity techniques in modern wireless communications, no work to-date has incorporated spatial diversity antennas in path-loss models. For example, the works in [8–12] presented path-loss models for MIMO systems; however these models do not have any term that accounts for the effect of the number of receiving diversity antennas. The author in [13] conducted spatial diversity measurement campaigns in a modern factory at 2.4 GHz to obtain path-loss models. However, there is no term in the presented path-loss models that accounts for the number of antenna elements. The work in [14] proposed a theoretical-based diversity gain model, which accounts for the number of antenna elements. However, since there is no distance-dependent term in the model, it is not like the traditional path-loss models in the literature.

Our previous works in [15, 16] proposed a receiver spatial diversity and a beam combining path-loss model, respectively, based on the log-distance model. However, since the floating intercept model (FIM) is also widely used in the literature, for example, in the 3GPP [17] and WINNER II [18] standards, which are widely utilized in multi-antenna-based systems, it becomes imperative to develop such a receiver spacial diversity model in accordance with these standards. This work proposes a receiver spatial diversity propagation path-loss channel model based on the FIM at 2.4 GHz. We present a comprehensive analysis of our path-loss measurement data that were collected in an indoor environment at 2.4 GHz. The proposed receiver spatial diversity models present terms that account for the effects of the number of receiving antenna elements in the path-loss equations.

The rest of this article is organized as follows. Section 2 discusses the equal gain power combining (EGC) procedure with the related combining types. Section 3 illustrates the experimental procedure and the LOS and NLOS propagation scenarios. Section 4 introduces the measurements-based path-loss channel models and analyzes them. Section 5 presents the proposed spatial diversity path-loss channel models and, finally, Section 6 summarizes the article.

2. Equal Gain Power Combining Procedure

In order to improve the performance of wireless link, we employ equal gain power combining (EGC) at the RX side. Two combining schemes are adopted in our work, the non-coherent combining (NCC) and the coherent combining (CC) each of which will combine the power of the received signals that arrive from the receiving diversity antennas. The potential enhancement that is achieved from these two schemes are quantitatively investigated by means of the average enhancement (i.e., reduction) in the path-loss and by means of the percentage of the path-loss exponent (PLE) reduction relative to the single antenna reception case (i.e., SISO system) as well as by means of cumulative distribution function (CDF). In CC scheme, the received powers from each RX diversity antenna are cophased and aligned, so they can be combined together using a known carrier phase information [1, 2, 5]. This enables us to extract the maximum power from each diversity antenna element. The NCC, on the other hand, assumes that signals phases from each individual receiving diversity antenna are independently and identically distributed (i.i.d). This means that we can directly linearly add the powers from each antenna without the need for any alignment or phase information [1, 2, 5]. The CC and NCC of the received spatial diversity powers, that is, $P_{r\mathrm{CC}}$ and $P_{r\mathrm{NCC}}$, are given, respectively, by [2]

$$P_{r\mathrm{CC}}(d) = \left(\sum_{i=1}^{N_r}\sqrt{P_i}\right)^2, \tag{1}$$

$$P_{r\mathrm{NCC}}(d) = \sum_{i=1}^{N_r} P_i, \tag{2}$$

where P_i is the received power in Watts and N_r is the number of receiving antenna elements. We used these two combining schemes on our measurement data, for power received from two, three, or more receiving diversity antennas. The corresponding log-distance and floating intercept propagation path-loss channel models are then developed for cases of line-of-site (LOS) and non-LOS (NLOS) propagation scenarios.

3. Experimental Procedure

3.1. Measurements Setup. The test signal that is used in our receiver spatial diversity indoor measurement campaigns is generated using the Warp v3 kit [19], similar to the experiments conducted in [15, 20]. In our experiments, we selected one LOS and one NLOS transmitter location and randomly selected nine LOS and nine NLOS locations scattered in an indoor, stationary, laboratory environment with TX-RX separation distances up to 9 m. Figure 1 shows the indoor lab environment along with the corresponding LOS and NLOS measurement locations. At each TX-RX LOS/NLOS location, one TX antenna and up to four RX antennas were used (i.e., 1×4 single-input multiple-output 1×4 SIMO system). Figure 2 shows the block diagram of the 1×4 receiver spatial diversity that is used in the measurement campaigns. MATLAB-based digital signal processing (DSP) tools are used to generate, transmit, receive, and process the radio signals. A PC-running MATLAB is connected to a 1 GB Ethernet switch, which links the TX and RX Warp v3 boards via an Ethernet switch. The rest of the

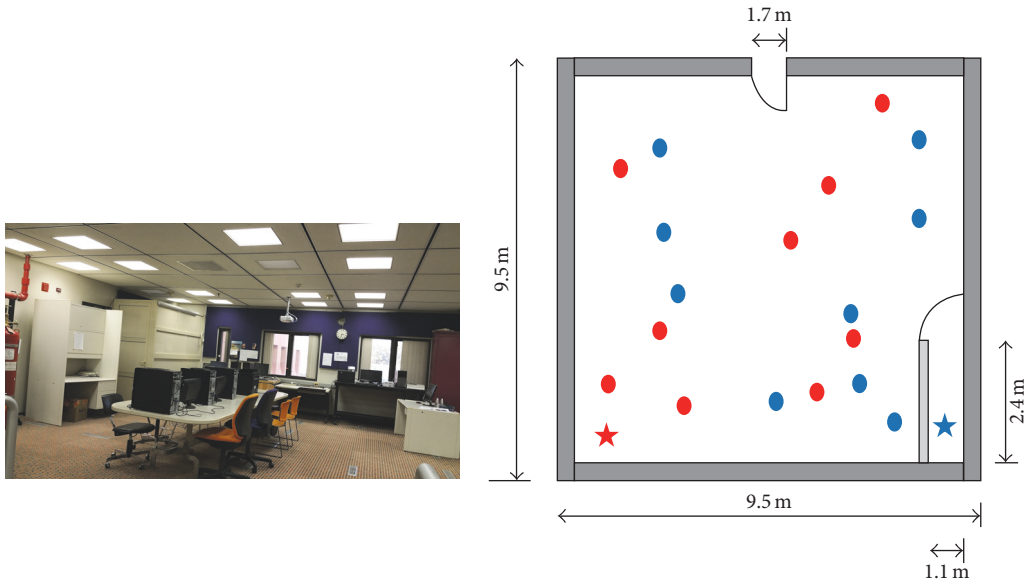

(a) Environment (b) Plan

FIGURE 1: The indoor lab in which the LOS (red points) and the NLOS (blue points) receiver spatial diversity power measurements have been conducted. The stars represent TX locations while the circles represent RX locations: (a) the actual environment and (b) the plan.

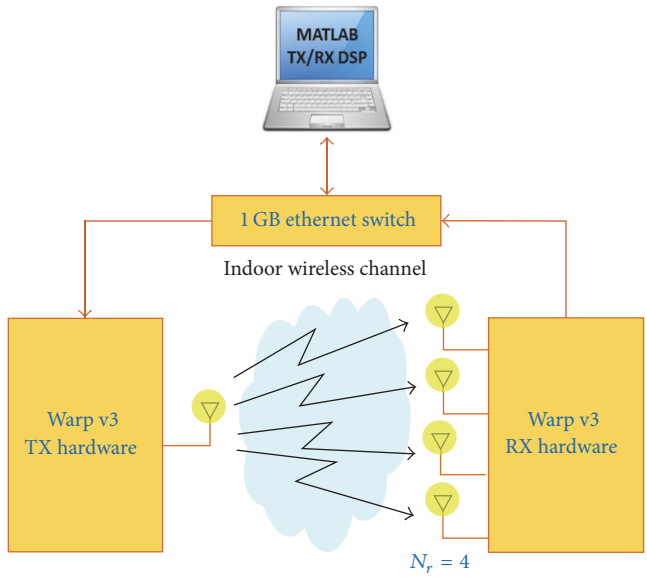

FIGURE 2: Block diagram of the 1×4 receiver spatial diversity path-loss measurement campaigns.

measurement parameters are documented in Table 1. During the measurements, we recorded ten power readings at each of the locations depicted in Figure 1(b), and the average of each antenna power reading is used in the data analysis to obtain the respective large-scale propagation path-loss channel models.

3.2. Scenarios Description. The indoor lab environment in which receiver spatial diversity path-loss measurement campaigns were conducted is shown in Figure 1(a). The walls are made of metals, the inner wall shown in Figure 1(a) is made of aluminum, and the ceiling is primarily made of iron while the ground is covered by carpet. In the middle of the lab there are a number of PCs, printers, tables, chairs, desks, office cabinets, and so forth as shown in Figure 1(a). These scatterers will be sources of diversity at the receiver side.

4. Large-Scale Propagation Path-Loss Models and Analysis

All wireless communication systems use large-scale propagation path-loss analysis as a key parameter in designing

Table 1: LDM parameters for SISO and SIMO cases using NCC and CC schemes when considering the LOS and NLOS scenarios along with the respective PLE reduction.

Parameter	Scenario	PLE (n)	STD (σ)	PLE reduction (%)
Single arbitrary antenna	NLOS	2.959	6.645	—
	LOS	2.105	3.652	—
Two antennas (NCC)	NLOS	2.242	3.66	24.25
	LOS	1.473	1.921	30.02
Two antennas (CC)	NLOS	1.888	3.332	36.22
	LOS	1.14	2.015	45.82
Three antennas (NCC)	NLOS	1.557	2.785	47.39
	LOS	1.042	2.723	50.47
Three Antennas (CC)	NLOS	1.034	2.536	65.06
	LOS	0.523	3.398	75.17
Four antennas (NCC)	NLOS	1.438	2.663	51.4
	LOS	0.926	2.845	55.98
Four antennas (CC)	NLOS	0.738	2.668	75.07
	LOS	0.223	3.873	89.4
Frequency (GHz)		2.4		
TX height (m)		1.5		
RX height (m)		1.5		
TX gain (dBi)		5		
RX gain (dBi)		5		
TX power (dBm)		−14		
Bandwidth (MHz)		20		

and deploying infrastructure. Information extracted from such analysis is widely used in link budget calculations, service coverage prediction, interference computation, and modulation and coding scheme (MCS) designs. The wireless channel path-loss is expressed in dB as a function of the distance between the TX and RX on a logarithmic scale. The most widely used models in characterizing the path-loss of wireless channels are the log-distance and the floating intercept path-loss channel models.

4.1. Log-Distance Path-Loss Models. The log-distance path-loss model (LDM) is given by [1, 15, 16, 21]

$$\mathrm{PL}(d)\,[\mathrm{dB}] = \mathrm{PL}_{\mathrm{dB}}(d_0) + 10n\log_{10}\left(\frac{d}{d_0}\right) + X_\sigma, \quad d \geq d_0, \tag{3}$$

where $\mathrm{PL}_{\mathrm{dB}}(d_0)$ is the path-loss at a reference distance d_0, n is the path-loss exponent (PLE), and X_σ is a zero mean Gaussian variable in dB with a standard deviation (also called shadow factor) given by σ in dB. The values of n and σ are calculated by finding the best minimum mean square error (MMSE) line fit to the empirical data. Next we apply the coherent combining CC (1) and noncoherent combining NCC schemes (2) to all the possible combinations of LOS and NLOS receiver diversity cases. The results are obtained for the single-input single-output (SISO), 1 × 2 SIMO, 1 × 3 SIMO, and 1 × 4 SIMO cases. During data analysis, antenna 1 is selected to represent the SISO case and it is considered as a reference for the quantitative analysis. Table 1 documents the resultant values of PLE and σ for all these schemes when considering the LOS and NLOS propagation scenarios. Figures 3, 4, and 5 plot these LDMs with respect to 1 m reference distance along with the respective measured scattered data for the cases of 1 × 2, 1 × 3, and 1 × 4 SIMO systems, respectively.

The performance of CC over that of NCC is obvious in all these figures and is quantitatively documented in Table 1 for each combining scheme. For instance, a reduction of 55.98% is achieved if we combine four received powers noncoherently in the LOS scenario, compared to 89.4% reduction in the same LOS scenario for the case of CC scheme. This performance superiority of CC over the NCC is already well established in the literature. It is also evident from Table 1 that a significant reduction in the PLE can be achieved going from two receiving antenna elements to four receiving antennas, as expected.

4.2. Floating Intercept Path-Loss Models. The floating intercept path-loss model (FIM) is used in the 3GPP [17] and WINNER II [18] sets of standards, and it is given by [22]

$$\mathrm{PL}(d)\,[\mathrm{dB}] = \alpha + 10\beta\log_{10}(d) + X_\sigma, \tag{4}$$

where α is the floating intercept in dB and β is the linear slope. The parameters of this model are obtained by applying the least-square linear regression fit to our measurement data in order to find the best-fit values of α and β with minimum

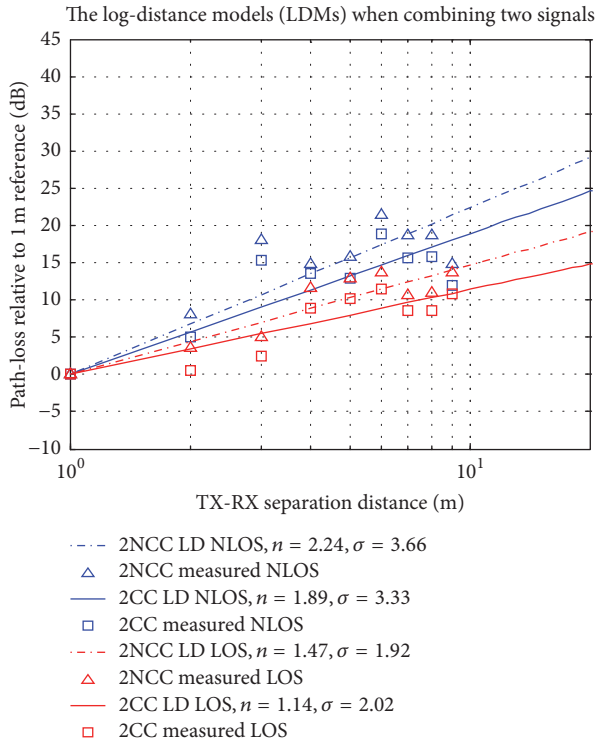

Figure 3: LDMs along with the measured scattered data when combining two signals coherently and noncoherently for the LOS and NLOS propagation scenarios.

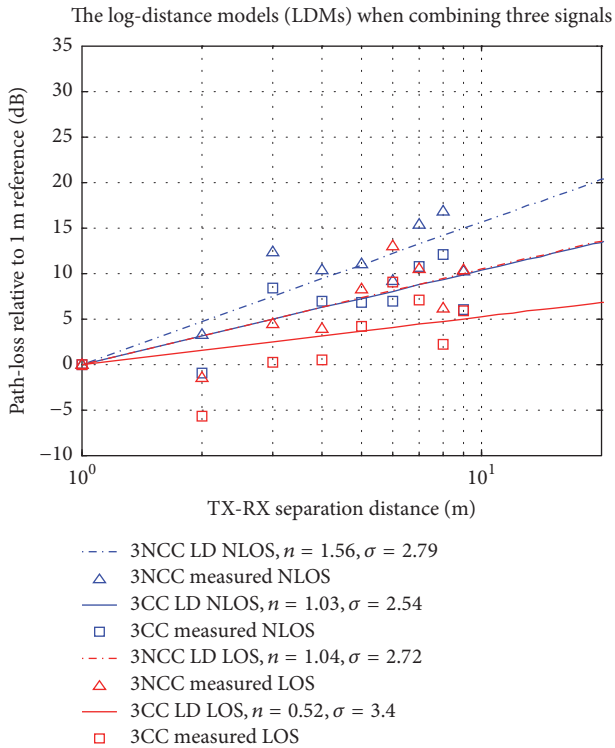

Figure 4: LDMs along with the measured scattered data when combining three signals coherently and noncoherently for the LOS and NLOS propagation scenarios.

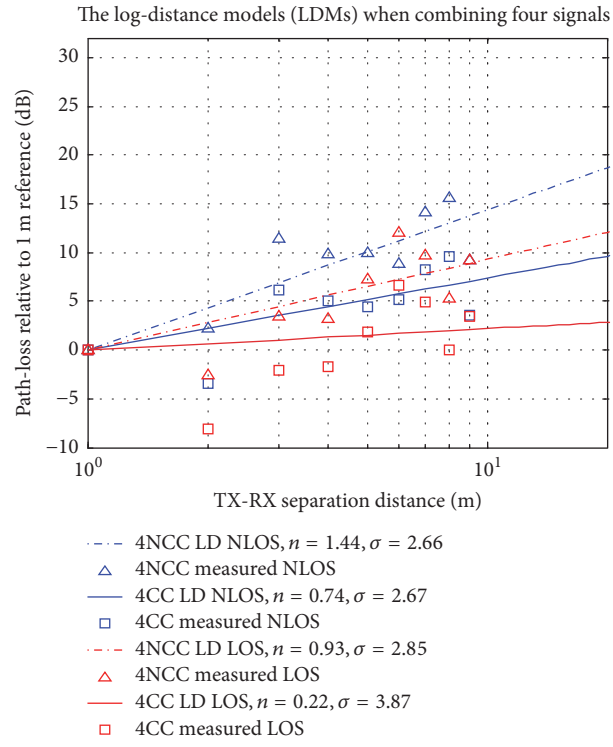

Figure 5: LDMs along with the measured scattered data when combining four signals coherently and noncoherently for the LOS and NLOS propagation scenarios.

standard deviation. This mathematical approach is explained in detail in [22]. Similarly, after applying the NCC and CC schemes to our receiver spatial diversity measurement data, we obtained the parameters of the FIM for all the possible combinations of LOS and NLOS receiver diversity cases. Table 2 documents the FIM parameters for cases of SISO, 1×2 SIMO, 1 × 3 SIMO, and 1 × 4 SIMO systems. Figures 6, 7, and 8 plot these FIMs along with the respective measured scattered data for the cases of 1 × 2, 1 × 3, and 1 × 4 SIMO systems, respectively. The advantage of using equal gain power combining techniques is also quantitatively presented in Table 2 by means of average path-loss enhancement (i.e., path-loss reduction) over the case of single antenna reception. Again, the performance of CC over the NCC scheme is evident as documented in Table 2. For example, combining the four signals powers coherently in a NLOS scenario will give an average path-loss enhancement of 16.82 dB compared to 11.45 dB for the same NLOS scenario when considering NCC. The advantages of using CC and NCC to combat path-loss and to enhance link quality can also be quantitatively investigated by means of cumulative distribution function (CDF) plots of the received signal powers. Figures 9 and 10 show CDF plots of the received powers for the LOS and NLOS scenarios, respectively, in which we can see the potentials of using CC and NCC to combat path-loss. For example, for the LOS scenario shown in Figure 9, around 90% of time the received signal power will be greater than −30 dBm if we combine four signals coherently compared to just around 10% of time if only one antenna was used. Similarly, in the CDF

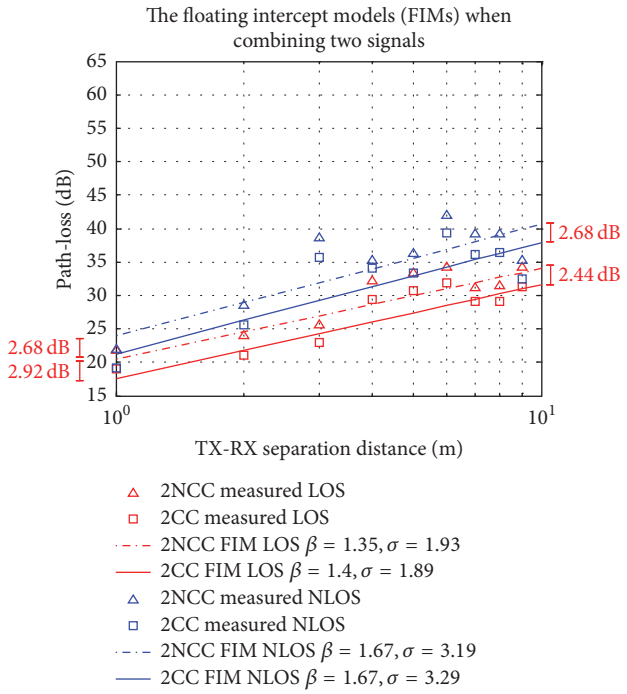

Figure 6: FIMs along with the scattered data for 1 × 2 SIMO case when considering CC and NCC for both the LOS and NLOS propagation scenarios.

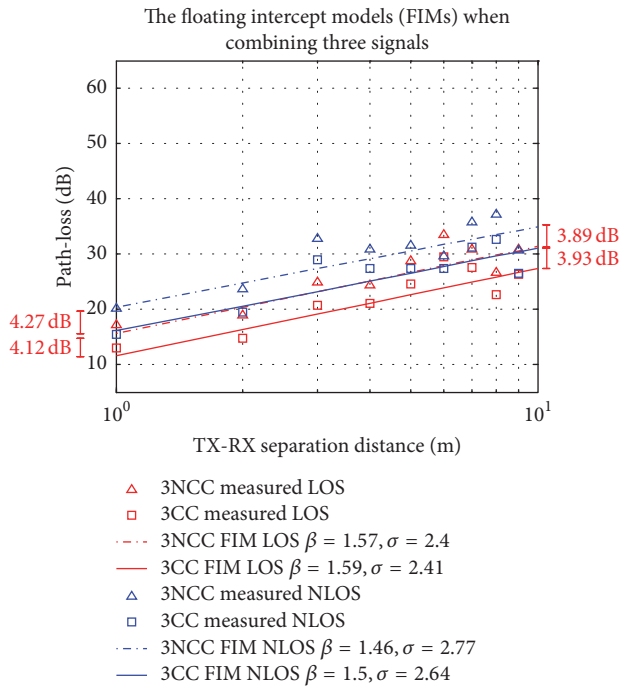

Figure 7: FIMs along with the scattered data for 1 × 3 SIMO case when considering CC and NCC for both the LOS and NLOS propagation scenarios.

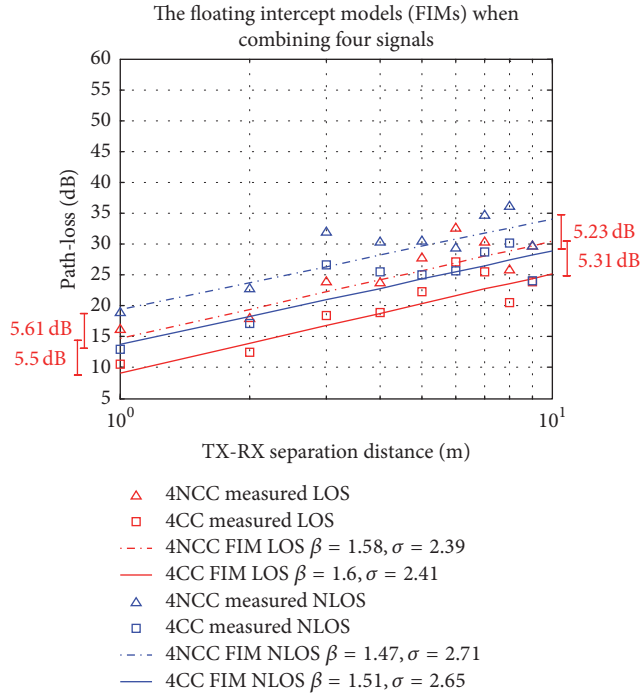

Figure 8: FIMs along with the scattered data for 1 × 4 SIMO case when considering CC and NCC for both the LOS and NLOS propagation scenarios.

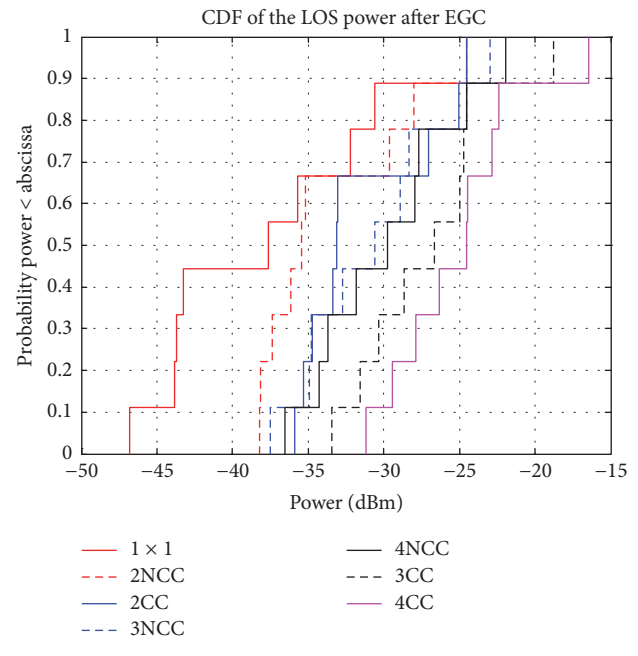

Figure 9: CDF of receiver spatial diversity after applying CC and NCC schemes for the LOS scenario.

plot of the NLOS case shown in Figure 10, around 90% of time the received signal power is greater than −34 dBm when combining four signals coherently compared to only 10% of time if only one antenna was used.

The reduction in path-loss achieved from both the NCC and CC schemes can be utilized by service providers to extend the service coverage area, which reflects the significance of this information.

Table 2: FIM parameters along with the average path-loss enhancements of receiver diversity for all the cases of SIMO reception.

Scenario	LOS							NLOS						
Combining type	NCC			CC				NCC			CC			
Diversity scheme	1 × 2	1 × 3	1 × 4	1 × 1	1 × 2	1 × 3	1 × 4	1 × 2	1 × 3	1 × 4	1 × 1	1 × 2	1 × 3	1 × 4
α [dB]	21.42	16.53	15.57	24.75	18.5	12.41	10.07	24.83	21.26	20.26	31.36	22.15	16.99	14.65
β	1.35	1.57	1.58	1.54	1.4	1.59	1.6	1.67	1.46	1.47	1.53	1.67	1.5	1.51
σ [dB]	1.93	2.4	2.39	3.81	1.89	2.41	2.41	3.19	2.77	2.71	5.21	3.29	2.64	2.65
Average enhancement in path-loss (dB)	4.52	8.08	8.98	—	7.11	12.06	14.34	5.6	10.53	11.45	—	8.32	14.56	16.82

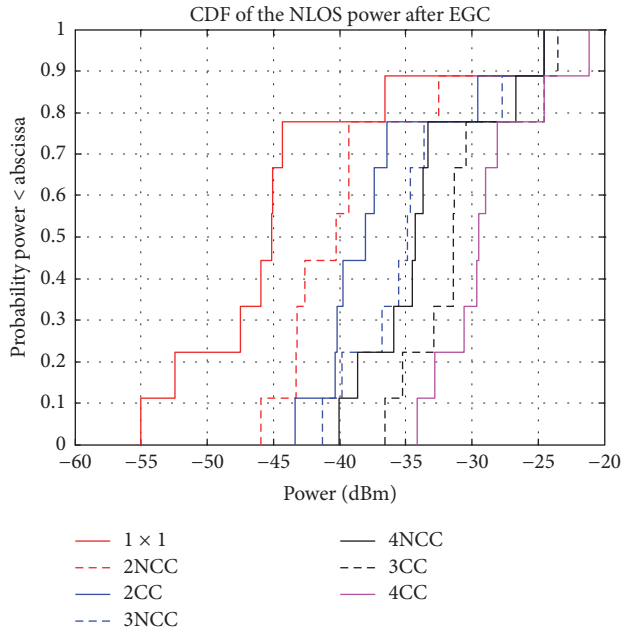

Figure 10: CDF of receiver spatial diversity after applying CC and NCC schemes for the NLOS scenario.

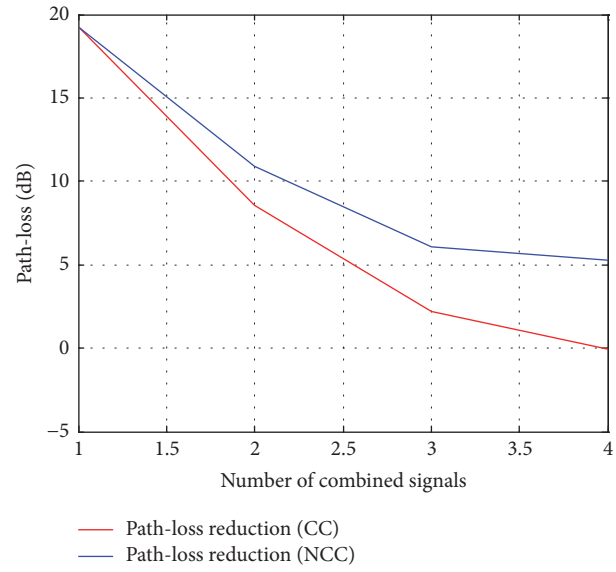

Figure 11: The logarithmic-like reduction in the path-loss values as the number of diversity antennas goes from one up to four at 8 m separation distance for the LOS scenario.

5. Receiver Spatial Diversity Propagation Path-Loss Channel Models

It was noticed that, at any TX-RX individual location, the path-loss values are reduced in a logarithmic manner as the number of diversity antenna elements being combined goes from one up to four, for both the NCC and CC schemes. This is depicted in Figure 11, which shows the path-loss reduction at 8 m separation distance for the NCC and CC schemes when considering the LOS propagation scenario. Furthermore, it is also evident from Figures 3–5 that the slope (or PLE) is reduced as a function of the number of combined signal powers. Therefore, we rely on these trends observed in our data to propose measurements-based spatial diversity propagation path-loss channel models that account for the number of receiving diversity antennas in the path-loss equations. The proposed diversity models are developed based on the log-distance path-loss model that is given by (3) and the floating intercept path-loss model that is given by (4). These models account for the number of antenna elements directly in the path-loss estimation.

The proposed log-distance-based diversity path-loss model is given by

$$\mathrm{PL}_{\mathrm{Div}}(d)\,[\mathrm{dB}] = \mathrm{PL}(d_0) + \left(10 n_{\mathrm{SISO}} \log_{10}\left(\frac{d}{d_0}\right)\right) \cdot \left(1 - A \log_2(N_r)\right) + X_\sigma, \tag{5}$$

while the floating intercept-based diversity path-loss model is given by

$$\mathrm{PL}_{\mathrm{Div}}(d)\,[\mathrm{dB}] = \alpha_{\mathrm{SISO}}\left(1 - B \log_2(N_r)\right) + 10\beta_{\mathrm{SISO}} \log_{10}(d) + X_\sigma, \tag{6}$$

where n_{SISO} is the PLE for a single antenna reception (SISO scheme), α_{SISO} is the floating intercept for the SISO case, β_{SISO} is the linear slope for the SISO case, N_r is the number of receiving diversity antenna elements, and A and B are weighting factors that are obtained by applying the MMSE fit (or least-square linear regression fit) to find the best-fit value to the measured data with minimum standard deviation. For the log-distance-based diversity model, the values of A are obtained by fixing the values of n_{SISO} and then performing the

MMSE fit in order to find the best values of A that give the corresponding measured values of PL and N_r, whereas, for the floating intercept-based diversity model, the respective values of B are determined by first fixing the values of α_{SISO} and β_{SISO} and then performing the MMSE fit to determine the best values of B that give the corresponding values of PL and N_r. The closed-form expressions used to find A and B along with their derivations are provided in Appendix. These approaches are used to obtain the values of A and B for both diversity models for the CC and NCC schemes when considering LOS and NLOS propagation scenarios. Table 3 documents the values of A and B for the two proposed diversity models that are given by (5) and (6). It is worth pointing out that the proposed diversity models given by (5) and (6) reduce to (3) and (4), respectively, when $N_r = 1$ (the SISO case), as would be required.

Next, we test the accuracy of the proposed diversity models to see how accurately they match the measured path-loss curves. Figures 12–15 compare the log-distance-based diversity path-loss model (5) with the measured log-distance model (3) for the CC and NCC when considering LOS propagation scenario. Figures 12 and 13 present these results for LOS scenarios for the CC and NCC, respectively, while Figures 14 and 15 present these results for NLOS scenarios for the CC and NCC, respectively. On the other hand, the accuracy of the floating intercept-based diversity model (6) is examined by comparing it with the measured floating intercept model (4). Figures 16–19 plot this diversity model against the measured floating intercept models for the CC and NCC schemes when considering LOS scenario. Figures 16 and 17 present these results for LOS scenario for the CC and NCC, respectively, while Figures 18 and 19 present these results for NLOS scenario for the CC and NCC, respectively.

It is evident from all these figures that the proposed diversity path-loss models match the measured path-loss models fairly well for all the CC and NCC schemes when considering the LOS and NLOS scenarios, after applying the appropriate values of the weighting factors A and B.

The proposed receiver spatial diversity propagation path-loss models given by (5) and (6) are quite useful. This is due to their ability to estimate or predict the path-loss values even for the case when we combine more than four signals (i.e., $N_r > 4$), given that we are considering the same measurement parameters (i.e., carrier frequency, operating environment, propagation scenario, and TX/RX heights). All what one needs is to choose the appropriate values of diversity models' parameters from Tables 1, 2, and 3 (i.e., A, B, n_{SISO}, α_{SISO}, and β_{SISO}) and the diversity models can estimate the path-loss values for the case $N_r > 4$. For example, using the floating intercept-based diversity model given by (6) one would use $\alpha_{\text{SISO}} = 31.36$ and $\beta_{\text{SISO}} = 1.53$ along with $B = 0.276$ from Tables 2 and 3, respectively, to estimate the path-loss for NLOS CC case when combining $3, 5, 7$, and 10 signals given that we have the same measurement parameters. Figure 20 shows the path-loss prediction for this case. For the respective case but with using the log-distance-based diversity model given by (5), one would use $n_{\text{SISO}} = 2.959$ along with $A = 0.385$ from Tables 1 and 3 in which similar trends to those shown in Figure 20 would be observed. Another advantage of the proposed general diversity path-loss models given by (5) and (6) is that they require less number of parameters calculations for any arbitrary number of coherently/noncoherently combined signals N_r. For example, consider the case if we try to combine sixteen signals either coherently or noncoherently. When using the floating intercept-based general diversity model (6),

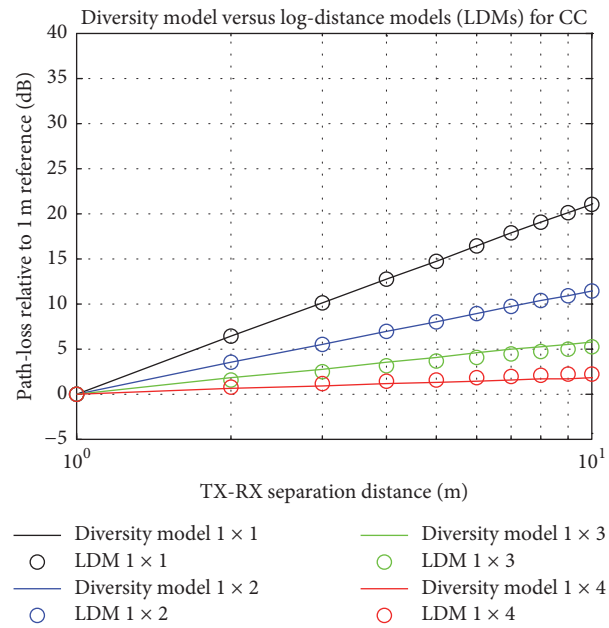

Figure 12: Path-loss for the proposed log-distance-based diversity model given by (5) for the CC scheme when considering LOS scenario, with $n_{\text{SISO}} = 2.105$ and $A = 0.458$.

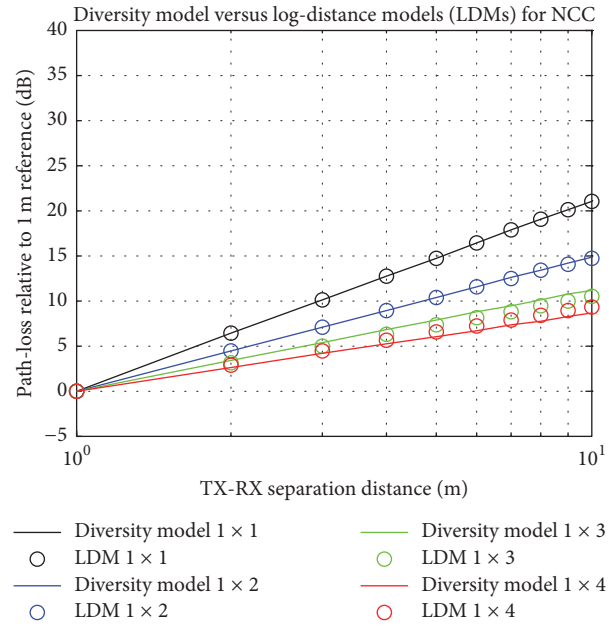

Figure 13: Path-loss for the proposed log-distance-based diversity model given by (5) for the NCC scheme when considering LOS scenario, with $n_{\text{SISO}} = 2.105$ and $A = 0.296$.

Table 3: Parameters of the proposed receiver spatial diversity path-loss models presented in (5) and (6).

Diversity model	Log-distance-based diversity model				Floating intercept-based diversity model			
Scenario	LOS		NLOS		LOS		NLOS	
Combining scheme	NCC	CC and SISO	NCC	CC and SISO	NCC	CC and SISO	NCC	CC and SISO
A	0.296	0.458	0.269	0.385	—	—	—	—
B	—	—	—	—	0.189	0.295	0.192	0.276
σ [dB]	3.777	4.051	5.89	3.174	2.32	2.75	3	3.65

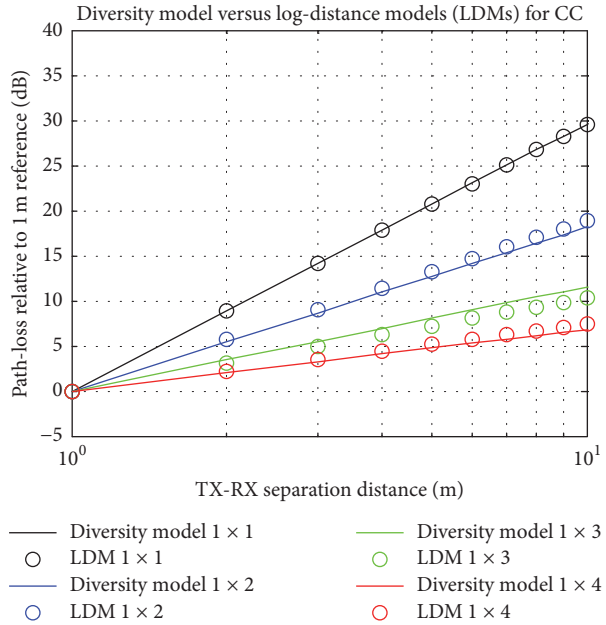

Figure 14: Path-loss for the proposed log-distance-based diversity model given by (5) for the CC scheme when considering NLOS scenario, with $n_{SISO} = 2.959$ and $A = 0.385$.

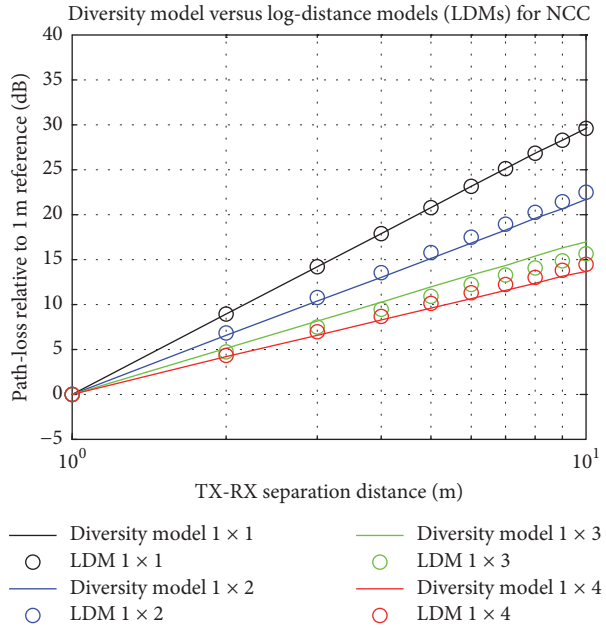

Figure 15: Path-loss for the proposed log-distance-based diversity model given by (5) for the NCC scheme when considering NLOS scenario, with $n_{SISO} = 2.959$ and $A = 0.269$.

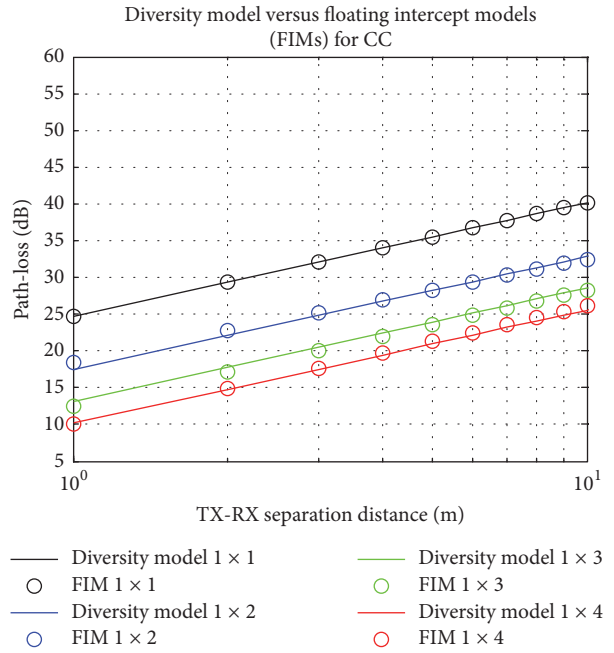

Figure 16: Path-loss for the proposed floating intercept-based diversity model given by (6) for the CC scheme when considering LOS scenario, with $\alpha_{SISO} = 24.75$, $\beta_{SISO} = 1.54$, and $B = 0.295$.

instead of calculating thirty-two parameters (sixteen for α and another sixteen for β) in the standard FIM, we only require to calculate three parameters in the proposed diversity model, which are B, α_{SISO}, and β_{SISO}. This means that the proposed diversity model is using only three values to replace thirty-two values with a very good accuracy in the path-loss estimates as shown in Figures 16–19 for our case. For the respective case but with using the log-distance-based diversity model (5), we only require to find two parameters in the proposed diversity model, which are A and n_{SISO} instead of finding sixteen values of the PLE in the standard log-distance model. This means that the proposed diversity model is using only two values to replace sixteen values with a very good accuracy in the path-loss estimates as shown in Figures 12–15 for our case. The proposed receiver spatial diversity path-loss channel models can thus be used in modern wireless systems to account for the general number of receiving diversity antennas in the path-loss calculation.

6. Conclusion

In this paper we propose receiver spatial diversity propagation path-loss channel models. These models are developed

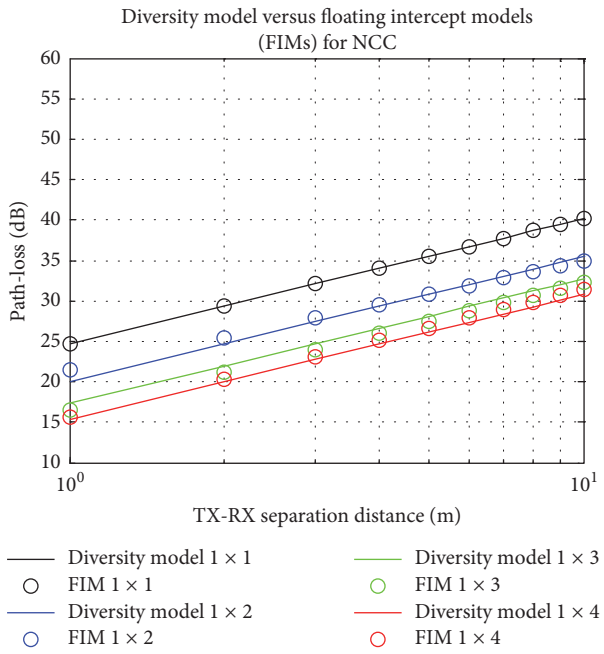

Figure 17: Path-loss for the proposed floating intercept-based diversity model given by (6) for the NCC scheme when considering LOS scenario, with $\alpha_{SISO} = 24.75$, $\beta_{SISO} = 1.54$, and $B = 0.189$.

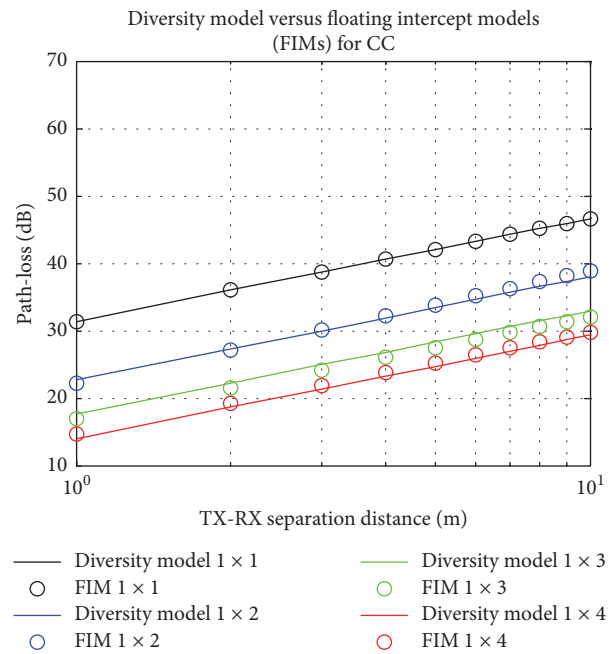

Figure 18: Path-loss for the proposed floating intercept-based diversity model given by (6) for the CC scheme when considering NLOS scenario, with $\alpha_{SISO} = 31.36$, $\beta_{SISO} = 1.53$, and $B = 0.276$.

from real-field measurement campaigns conducted in an indoor lab environment for LOS and NLOS propagation scenarios at 2.4 GHz. The proposed diversity models are developed based on the well-known log-distance and floating intercept models and they incorporate the number of receiving diversity antennas directly in the path-loss estimation. We quantitatively illustrated the advantage of using equal gain coherent and noncoherent power combining (i.e., CC and NCC) to reduce the path-loss by means of the percentage of PLE reduction and in terms of the average enhancement in path-loss as well as by means of cumulative distribution function (CDF). It is shown that combining four signals coherently in a LOS scenario will result in a PLE reduction of 89.4% compared to 55.98% reduction if using NCC for the same LOS scenario. The proposed spatial diversity path-loss models can account for the effect of the general number of receiving diversity antenna elements in the path-loss equations. Our future work in this field is to extend these measurement campaigns to the millimeter wave band, both in indoor and in outdoor environments.

Appendix

In this section we provide mathematical derivations for the formulas used to obtain the values of the two weighting factors A and B given by (5) and (6), respectively. The objective is to find the values of A and B that minimize the mean square error between the measured path-loss values and the predicted values using the spatial diversity models in (5) and (6), respectively.

A. Log-Distance-Based Diversity Path-Loss Model

Let $\mathrm{PL}(d)$ be the measured path-loss values and let $J(A)$ be the objective function to be minimized; that is,

$$J(A) = \sum_{i=1}^{N_{CC},N_{NCC}} \left[\mathrm{PL}(d_i) - \mathrm{PL}_{Div}(d_i)\right]^2,$$

$$J(A) = \sum_{i=1}^{N_{CC},N_{NCC}} \left[\mathrm{PL}(d_i) - \mathrm{PL}(d_0) - 10n_{SISO}\log_{10}\left(\frac{d_i}{d_0}\right) + 10An_{SISO}\left(\frac{d_i}{d_0}\right)\log_2(N_i)\right]^2. \quad (A.1)$$

Let $a_i = \mathrm{PL}(d_i) - \mathrm{PL}(d_0) - 10n_{SISO}\log_{10}(d_i/d_0)$, and we get

$$J(A) = \sum_{i=1}^{N_{CC},N_{NCC}} \left[a_i + 10An_{SISO}\log_{10}\left(\frac{d_i}{d_0}\right)\log_2(N_i)\right]^2. \quad (A.2)$$

Now find $d(J(A))/d(A) = 0$ and arrange the equation; we get

$$\sum_{i=1}^{N_{CC},N_{NCC}} \log_{10}\left(\frac{d_i}{d_0}\right)\log_2(N_i) \cdot \left[a_i + 10An_{SISO}\log_{10}\left(\frac{d_i}{d_0}\right)\log_2(N_i)\right] = 0. \quad (A.3)$$

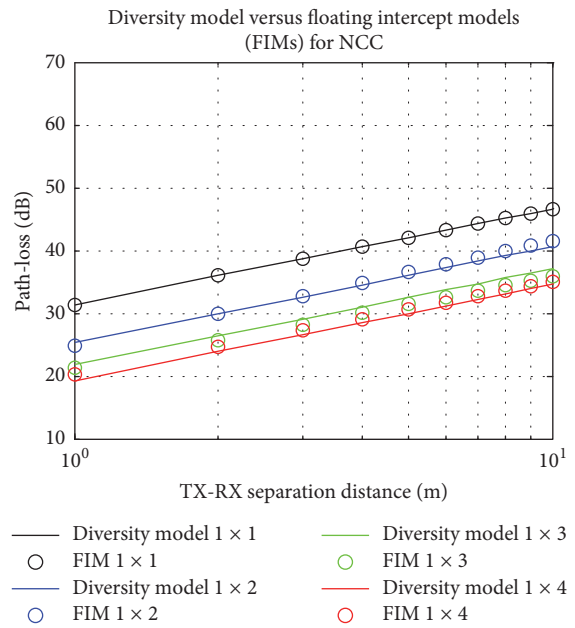

Figure 19: Path-loss for the proposed floating intercept-based diversity model given by (6) for the NCC scheme when considering NLOS scenario, with $\alpha_{\text{SISO}} = 31.36$, $\beta_{\text{SISO}} = 1.53$, and $B = 0.192$.

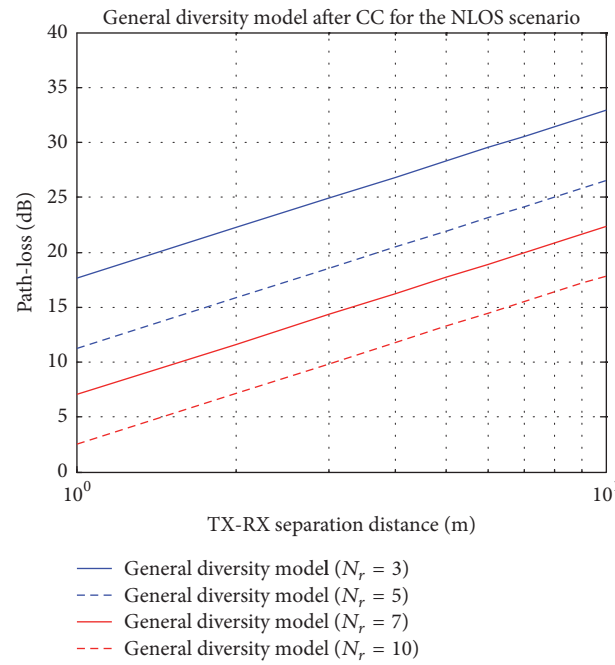

Figure 20: Path-loss prediction for arbitrary number of combined signals using the proposed general receiver diversity path-loss model given by (6), for the NLOS CC case with $\alpha_{\text{SISO}} = 31.36$ and $\beta_{\text{SISO}} = 1.53$ along with $B = 0.276$ from Tables 2 and 3, respectively.

Solving for A we get the final formula as

$$A = \frac{-\sum_{i=1}^{N_{\text{CC}},N_{\text{NCC}}} \log_{10}(d_i/d_0)\log_2(N_i) * [a_i]}{10n_{\text{SISO}}\sum_{i=1}^{N_{\text{CC}},N_{\text{NCC}}} (\log_{10}(d_i/d_0))^2 (\log_2(N_i))^2}. \quad \text{(A.4)}$$

B. Floating Intercept-Based Diversity Path-Loss Model

Similarly,

$$J(B) = \sum_{i=1}^{N_{\text{CC}},N_{\text{NCC}}} [\text{PL}(d_i) - \text{PL}_{\text{Div}}(d_i)]^2,$$

$$J(B) = \sum_{i=1}^{N_{\text{CC}},N_{\text{NCC}}} [\text{PL}(d_i) - \alpha_{\text{SISO}} + B\alpha_{\text{SISO}}\log_2(N_i) - 10\beta_{\text{SISO}}\log_{10}(d_i)]^2. \quad \text{(B.1)}$$

Let $a_i = \text{PL}(d_i) - \alpha_{\text{SISO}} - 10\beta_{\text{SISO}}\log_{10}(d_i)$, and we get

$$J(B) = \sum_{i=1}^{N_{\text{CC}},N_{\text{NCC}}} [a_i + B\alpha_{\text{SISO}}\log_2(N_i)]^2. \quad \text{(B.2)}$$

Now find $d(J(B))/d(B) = 0$ and arrange the equation; we get

$$\sum_{i=1}^{N_{\text{CC}},N_{\text{NCC}}} [a_i\log_2(N_i) + \alpha_{\text{SISO}}B(\log_2(N_i))^2] = 0. \quad \text{(B.3)}$$

Solving for B we get the final formula as

$$B = \frac{-\sum_{i=1}^{N_{\text{CC}},N_{\text{NCC}}} \log_2(N_i) * [a_i]}{\alpha_{\text{SISO}}\sum_{i=1}^{N_{\text{CC}},N_{\text{NCC}}} (\log_2(N_i))^2}. \quad \text{(B.4)}$$

Conflicts of Interest

The authors declare that they have no conflicts of interest.

Acknowledgments

The project was supported by King Saud University, Deanship of Scientific Research, College of Engineering Research Center.

References

[1] T. S. Rappaport, *Wireless Communications: Principles and Practice*, Prentice Hall, Upper Saddle River, NJ, USA, 2nd edition, 2002.

[2] D. G. Brennan, "Linear diversity combining techniques," *Proceedings of the IEEE*, vol. 91, no. 2, pp. 331–356, 2003.

[3] A. I. Sulyman and M. Kousa, "Bit error rate performance of a generalized diversity selection combining scheme in Nakagami fading channels," in *Proceedings of the IEEE Wireless Communications and Networking Conference (WCNC '00)*, vol. 3, pp. 1080–1085, IEEE, September 2000.

[4] I. S. Ansari, F. Yilmaz, M.-S. Alouini, and O. Kucur, "New results on the sum of gamma random variates with application to the performance of wireless communication systems

over nakagami-m fading channels," *Transactions on Emerging Telecommunications Technologies*, vol. 28, no. 1, Article ID e2912, 2017.

[5] H. H. Beverage and H. O. Peterson, "Diversity receiving system of R.C.A. communications, inc., for radiotelegraphy," *Proceedings of the Institute of Radio Engineers*, vol. 19, no. 4, pp. 529–561, 1931.

[6] K. T. Herring, J. W. Holloway, D. H. Staelin, and D. W. Bliss, "Path-Loss characteristics of urban wireless channels," *IEEE Transactions on Antennas and Propagation*, vol. 58, no. 1, pp. 171–177, 2010.

[7] H. Kdouh, C. Brousseau, G. Zaharia, G. Grunfelder, and G. El Zein, "Measurements and path loss models for shipboard environments at 2.4 GHz," in *Proceedings of the IEEE 2011 41st European Microwave Conference (EuMC '11)*, pp. 408–411, October 2011.

[8] X. Zhao, B. M. Coulibaly, X. Liang et al., "Comparisons of channel parameters and models for urban microcells at 2 GHz and 5 GHz [wireless corner]," *IEEE Antennas and Propagation Magazine*, vol. 56, no. 6, pp. 260–276, 2014.

[9] V. Erceg, P. Soma, D. S. Baum, and S. Catreux, "Multiple-input multiple-output fixed wireless radio channel measurements and modeling using dual-polarized antennas at 2.5 GHz," *IEEE Transactions on Wireless Communications*, vol. 3, no. 6, pp. 2288–2298, 2004.

[10] Y. Wang, X.-L. Wang, Y. Qin, Y. Liu, W.-J. Lu, and H.-B. Zhu, "An empirical path loss model in the indoor stairwell at 2.6 GHz," in *Proceedings of the IEEE International Wireless Symposium (IWS '14)*, pp. 1–4, March 2014.

[11] J.-M. Molina-García-Pardo, J.-V. Rodríguez, and L. Juan-Llácer, "Polarized indoor MIMO channel measurements at 2.45 GHz," *IEEE Transactions on Antennas and Propagation*, vol. 56, no. 12, pp. 3818–3828, 2008.

[12] R. Mardeni and Y. Solahuddin, "Path loss model development for indoor signal loss prediction at 2.4 GHz 802.11n network," in *Proceedings of the International Conference on Microwave and Millimeter Wave Technology (ICMMT '12)*, vol. 2, pp. 724–727, May 2012.

[13] S. Phaiboon, "Space diversity path loss in a modern factory at frequency of 2.4 GHz," *WSEAS Transactions on Communications*, vol. 13, pp. 386–393, 2014.

[14] H.-G. Park, H. Keum, and H.-G. Ryu, "Path loss model with multipleantenna," in *Proceedings of the Progress in Electromagnetics Research Symposium*, pp. 2119–2124, Guangzhou, China, August 2014.

[15] A. Alwarafy, A. I. Sulyman, A. Alsanie, S. Alshebeili, and H. Behairy, "Receiver spatial diversity propagation path-loss model for an indoor environment at 2.4 GHz," in *Proceedings of the International Conference on the Network of the Future (NOF '15)*, pp. 1–4, October 2015.

[16] A. I. Sulyman, A. Alwarafy, G. R. MacCartney, T. S. Rappaport, and A. Alsanie, "Directional radio propagation path loss models for millimeter-wave wireless networks in the 28-, 60-, and 73-GHz bands," *IEEE Transactions on Wireless Communications*, vol. 15, no. 10, pp. 6939–6947, 2016.

[17] V6.1.0, 3GPP TR 25.996, Spatial channel model for multiple input multiple output MIMO simulations, September 2003.

[18] P. Kyösti, J. Meinilä, L. Hentilä et al., "D1. 1.2 WINNER II channel models part I channel models," Tech. Rep. IST-4-027756, WINNER Information Society Technologies, 2007.

[19] Mango Communications, http://mangocomm.com/products/kits/warp-v3-kit.

[20] K. M. Humadi, A. I. Sulyman, and A. Alsanie, "Experimental results for generalized spatial modulation scheme with variable active transmit antennas," in *Proceedings of the 10th International Conference on Cognitive Radio Oriented Wireless Networks (IEEE-Crowncom '15)*, Doha, Qatar, April 2015.

[21] A. Sulyman, A. Nassar, M. Samimi, G. Maccartney, T. Rappaport, and A. Alsanie, "Radio propagation path loss models for 5G cellular networks in the 28 GHZ and 38 GHZ millimeter-wave bands," *IEEE Communications Magazine*, vol. 52, no. 9, pp. 78–86, 2014.

[22] J. F. Kenney and E. S. Keeping, *Mathematics of Statistics*, van Nostrand, Princeton, NJ, USA, 1965.